Picosecond IR−UV Pump−Probe Spectroscopy. IVR of OH Stretching Vibration of Phenol and Phenol Dimer

Takayuki Ebata,* Masakazu Kayano, Shin Sato, and Naohiko Mikami*

Department of Chemistry, Graduate School of Science, Tohoku University, Sendai 980-8578, Japan

Received: March 20, 2001; In Final Form: June 12, 2001

Intramolecular and intracluster vibrational energy redistribution(IVR) from OH stretching vibrations of phenol and phenol dimer have been investigated for the first time by picosecond time-resolved IR−UV pump−probe spectroscopy. The OH stretching level was pumped by a picosecond IR laser pulse and the decay of the pumped level as well as appearance of the energy redistributed vibrational levels was observed using resonance enhanced multiphoton ionization scheme with a picosecond UV laser. For bare phenol, IVR of the OH stretching level was found to occur with a lifetime of 14 ps. For the dimer, a remarkable site-dependence was observed for the IVR lifetime of the OH stretching level; IVR of the proton-donating site occurs less than 5 ps, while that of the proton accepting site occurs with 14 ps, comparable to that of bare phenol. In the case of a cluster, IVR was followed by vibrational predissociation, which occurs with lifetimes of several tens of picoseconds.

Introduction

Recently, several double resonance spectroscopic techniques have been successfully applied to measure the OH stretching vibration of size-selected hydrogen-bonded (H-bonded) clusters of aromatic molecules, which has helped us substantially in the determination of their structures.[1−24] In these spectra, H-bonded OH stretching vibration exhibits characteristic lower-frequency shift depending on the H-bonding strength and the structure. The cluster structures are then determined by the analysis of the observed spectra with an aid of ab initio molecular orbital calculations.

Besides the characteristic shifts, OH stretching vibration often exhibits a large broadening in the H-bonded clusters.[3,5,9,12,13,24] The broadening of OH stretching vibration is well-known in the condensed phase, which is essentially explained by a heterogeneous broadening due to an overlap of the transitions of the OH groups in different environment as well as hot bands, and a homogeneous broadening due to dynamics of OH stretching vibration involving dephasing and population decay. The H-bonded cluster formed in supersonic jets may be an ideal system to investigate such the dynamics. In the jet, each cluster forms a specific structure and they are populated mostly in the zero-point vibrational level. So, by removing the inhomogeneous contribution, we can examine purely the coupling between OH stretching vibration and the intermolecular mode for the well-characterized H-bonded system.

Two spectroscopic methods can be used to investigate the vibrational dynamics of molecules and clusters. One is the frequency domain approach, such as high-resolution vibrational spectroscopy.[25−34] The high-resolution vibrational spectroscopy has been extensively applied to the clusters of diatomic molecules or small polyatomic molecules, such as $(HF)_n$, $(HCN)_n$, $(H_2O)_n$, etc.[30−34] In these clusters, a remarkable mode dependence was observed in vibrational predissociation (VP) lifetime. For example, in $(HF)_2$, the VP lifetime of the H-bonded HF stretch vibration ($\tau_{VP} = 0.48$ ns) is 40 times shorter than that of free HF ($\tau_{VP} = 20$ ns),[32] which clearly shows the non-RRKM behavior. These studies have provided detailed information on the coupling between the high-frequency mode and the dissociation continuum of the H-bonded clusters of small molecules, where intramolecular mode is not important. On the other hand, in case of the clusters of large polyatomic molecules, there are many intramolecular modes which are effective bath modes for the energy redistribution. These intramolecular modes will be more important in the dynamics of the clusters of aromatic molecules, since the intramolecular vibrational redistribution (IVR) is known to be very efficient even at small internal energy. For the clusters of aromatic molecules, the investigation of their dynamics by high-resolution vibrational spectroscopy is very complicated because of small rotational constants and low symmetry, resulting in the difficulty of extracting dynamics from the spectra.

The alternative approach is the real time observation of the dynamics by using the picosecond pump−probe method. One can directly obtain the time scale of IVR and VP, and can elucidate the pathway of the energy flow among the vibrational modes. This methodology has been extensively used to investigate IVR dynamics of molecules and clusters in the electronically excited state (S_1).[35−44] However, corresponding measurements for the electronically ground state (S_0) molecules or clusters are very few because of the experimental difficulty. Especially for the OH stretching vibration, to the best of our knowledge, time domain measurement has not been carried out yet either in the ground or in the electronically excited state.

In the present work, we present the first picosecond time-resolved measurement for the intramolecular or intracluster vibrational energy redistribution (IVR) of OH stretching of phenol and its dimer in the S_0 state. The structures of phenol and its clusters have been investigated in detail.[1−3,45−51] In addition, the dynamics of their electronically excited states were also studied by many groups.[52−61] On the other hand, corresponding studies on the dynamics in the S_0 state are very few.[62−64] Very recently, we carried out IR−UV pump−probe

* Authors to whom correspondence should be addressed.

10.1021/jp011043k CCC: $20.00
Published on Web 09/01/2001

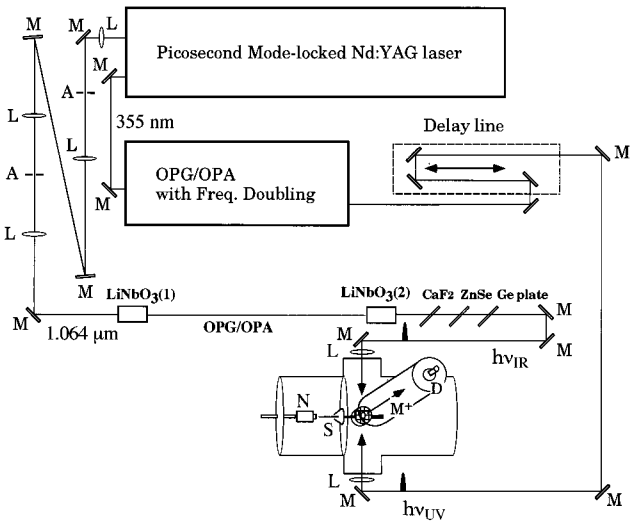

Figure 1. Experimental set up of picosecond IR− UV pump−probe spectroscopy. A: aperture. L: lens. M: mirror. D: detector. N: nozzle. S: skimmer. M^+: ion.

spectroscopy with nanosecond lasers,[65] and reported that IVR of OH stretching level of bare phenol occurred with a few nanoseconds and its decay profile was interpreted by an intermediate coupling scheme, while the clusters exhibited a statistical coupling limit behavior. However, the obtained lifetimes were very close to or shorter than the pulse duration of the lasers used. In addition, the lifetimes were much longer than those expected from the bandwidth measurement reported by the group of Felker.[52] So, a question occurred whether the observed time profile with nanosecond laser pulses shows a true dynamics of the OH stretching vibration.

To answer the above question, we have carried out a picosecond time-resolved IR−UV pump−probe spectroscopy study. In this work, the OH stretching level was prepared by a picosecond IR pulse and the decay of the pumped level as well as the appearance of the energy redistributed levels was monitored using resonance-enhanced multiphoton ionization with a picosecond UV pulse. We first measure IVR for OH stretching level of bare phenol, and then extend our investigation to phenol dimer. In the case of the dimer, there are two different OH groups; the H-bonded OH (so-called donor OH stretch) and the OH free from the H-bond (acceptor OH stretch). We can examine the difference of the coupling strength between OH stretching level and intermolecular modes for the two different sites of OH stretching level by measuring their IVR rates. In addition, energies of both OH vibrations are large enough to break the H-bond, which enables us to investigate the time scale of the vibrational predissociation (VP) after the energy randomization. This paper reports the first experimental result of the picosecond time-resolved IR−UV pump−probe spectroscopy for the H-bonded clusters in the electronic ground state.

Experimental Section

Figure 1 shows the experimental setup of picosecond IR−UV pump−probe spectroscopy. The setup consists of three parts: a mode-locked picosecond Nd^{3+}:YAG laser, an optical parametric generation (OPG)/optical parametric amplification (OPA) system with second harmonic generation, and an OPG/OPA system for tunable IR pulse generation. A fundamental output (1.064 μm) of the mode-locked picosecond Nd^{3+}:YAG laser (Ekspra PL2143B) is split into two. The major part is frequency tripled, and is introduced into an OPG/OPA system (Ekspra PG401SH) for the generation of a tunable UV light. A partially reflected 1.064 μm output is used to generate tunable IR output with a homemade OPG/OPA system, which consists of two $LiNbO_3$ crystals which are separated by 1 m. The 1.064 μm light is introduced into the first crystal placed on a rotational stage for the generation of broad band tunable IR light by OPG. The generated IR and 1.064 μm light beams are coaxially introduced into the second $LiNbO_3$ crystal placed on another rotational stage whose tuning angle is synchronized with that of the first crystal. The second crystal is used for amplification (OPA) as well as for narrowing of the IR bandwidth. After passing through the second crystal, both the signal(1.6 μm) and the idler (3 μm) lights are generated. CaF_2, ZnSe, and Ge plates are used to separate the signal and the 1.064 μm lights from the idler light. The finally obtained tunable IR light at 3 μm has a bandwidth of 10−15 cm^{-1} and an output power of 50−100 μJ, both of which are dependent on the wavelength.

Jet-cooled phenol was generated by a supersonic expansion of phenol vapor seeded in He carrier gas into vacuum through a pulsed nozzle (General valve) having a 0.8 mm aperture. Phenol was heated to 40 °C to obtain a sufficient vapor pressure. The jet-cooled phenol and clusters were skimmed by a skimmer (0.8 mm diameter Beam dynamics) located at 30 mm down stream of the nozzle. The IR and UV lasers were introduced into a vacuum chamber coaxially in a counterpropagating manner, and crossed the supersonic beam at 50 mm down stream of the skimmer. The molecules in the supersonic beam were ionized by 1+1 resonance enhanced MPI(REMPI) via S_1, and the ions were repelled to the direction perpendicular to the plane of the molecular beam and the laser beams. The ions were then mass-analyzed by a 50 cm time-of-flight tube and were detected by an electron multiplier (Murata Ceratron). The transient profiles of the pump−probe ion signals were observed by changing a delay time between UV and IR pulses by a computer-controlled optical delay line. The ion signals were integrated by a boxcar integrator (Par model 4420/4400) and processed by a microcomputer. Phenol was purchased form Wako chemical and was purified by vacuum sublimation before use.

Results and Discussion

We first examined the temporal widths of the picosecond IR and UV light pulses by deconvolution of the IR−UV pump−probe signal of the CH stretching vibration (ν_{CH}) of benzene.[54] The excitation scheme is shown as an inset of Figure 2, and Figure 2a shows the ionization-detected IR gain spectrum of benzene for the CH stretching vibration (ν_{20}). In this measurement, the UV pulse was introduced at a delay time of 30 ps after the IR pulse. The vibrational spectrum was obtained by scanning the IR frequency while monitoring the benzene ion, where the UV laser frequency was fixed to the $6_0^1 20_1^1$ transition (38650 cm^{-1}).[65] The peak at 3050 cm^{-1} (ν_{20}) is appeared by 1+1 REMPI with the UV light. Then we fixed the IR and UV frequencies to the ν_{20} vibration and to the $6_0^1 20_1^1$ electronic transition, respectively, and measured the appearance of the $6_0^1 20_1^1$ REMPI signal by changing the delay time between UV and IR pulses. Figure 2b shows a plot of the $6_0^1 20_1^1$ REMPI signal versus the delay time. As seen in Figure 2b, the $6_0^1 20_1^1$ REMPI signal increases up to 20 ps and approaches to a constant value. The simulated curve well reproduced the observed rise when we assumed both the IR and UV pulses have a Gaussian shape with fwhm of 14 ps, as is shown by the solid curve in Figure 2b. The pulse shapes for the IR and the UV lights were used for the analyses of the transient profiles of phenol and its dimer.

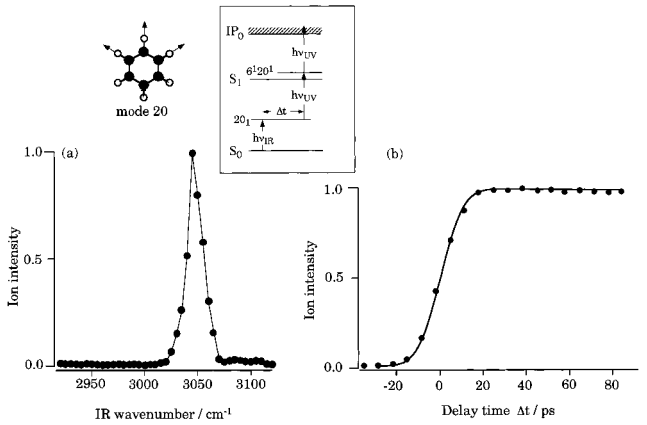

Figure 2. (a)IR spectrum of benzene in the CH stretching vibration (mode 20) obtained by scanning IR frequency while monitoring the 2 $0_1^1 6_0^1$ (1+1) REMPI signal. (b)Time profile of the $6_0^1 20_1^1$ band obtained by changing the delay time between IR and UV lasers. Here, the IR and UV frequencies are fixed to mode 20 and the $6_0^1 20_1^1$ transition, respectively. The solid curve is the convoluted curve obtained by setting the pump ($h\nu_{IR}$) and probe($h\nu_{UV}$) pulses to be 14 ps (fwhm) Gaussian pulses.

TABLE 1: Vibrational Frequencies (ν_{OH}), IVR Rate Constants (k_{IVR}), VP Rate Constants (k_{diss}), and Band Widths (Δ) of the OH Stretching Vibration of Bare Phenol and Phenol Dimer

ν_{OH}(cm^{-1})	k_{IVR}($\times 10^{11}$ s^{-1})	k_{diss}($\times 10^{10}$ s^{-1})	Δ(cm^{-1})[a]	Δ(cm^{-1})[b]
phenol				
3657	0.71		0.38	0.7
phenol dimer				
3654(A)	0.71	1.8	0.38	1.2
3530(D)	≥2	1.1	1.1	2.4

[a] Width obtained by using an equation $\Delta = (2\pi c)^{-1} k_{IVR}$. [b] Hartland et al. (ref 63).

1. Bare Phenol. Frequencies of the OH stretching vibration of bare phenol and phenol dimer are reported in our previous work[2,3] and the vibrational frequencies are listed in Table 1. The excitation and the monitoring scheme is shown in an inset of Figure 3. Phenol is excited to the OH stretching level by the IR pulse and the decay of the pumped level due to IVR and the appearance of the energy redistributed vibrational levels are monitored by 1+1 REMPI through the S_1 state with the UV pulse at different delay times. The S_1-S_0 spectrum from the OH stretching level exhibits sharp bands, while that of the energy redistributed levels (v") exhibits broad band because of the heavy congestion of many v′−v" transitions.

Figure 3a shows the 1+1 REMPI spectra of phenol measured at delay times of 10 and 200 ps after the IR excitation to OH stretching level. At the delay time of 10 ps, the spectrum consists of several sharp peaks and weak structure-less broad background in the higher frequency region. Among the several sharp bands, those at 32690, 33470, and 33630 cm^{-1} are assigned to $\nu_{OH_1}^0$, $\nu_{OH_1}^0 1_0^1$ and $\nu_{OH_1}^0 12_0^1$ transitions, respectively. At the 200 ps delay time, all the sharp bands diminish and the intensity of the broad background in the higher frequency region becomes prominent. The broad background is assigned to the transitions from the energy redistributed levels, and the disappearance of all the sharp peaks at 200 ps indicates that IVR is completed at this delay time. We then measured the transient behavior for each band.

Figure 3b shows the plots of the intensities of the $\nu_{OH_1}^0$ and $\nu_{OH_1}^0 12_0^1$ bands, and the broad background monitored at 33700 cm^{-1} as a function of the delay time between the IR and the

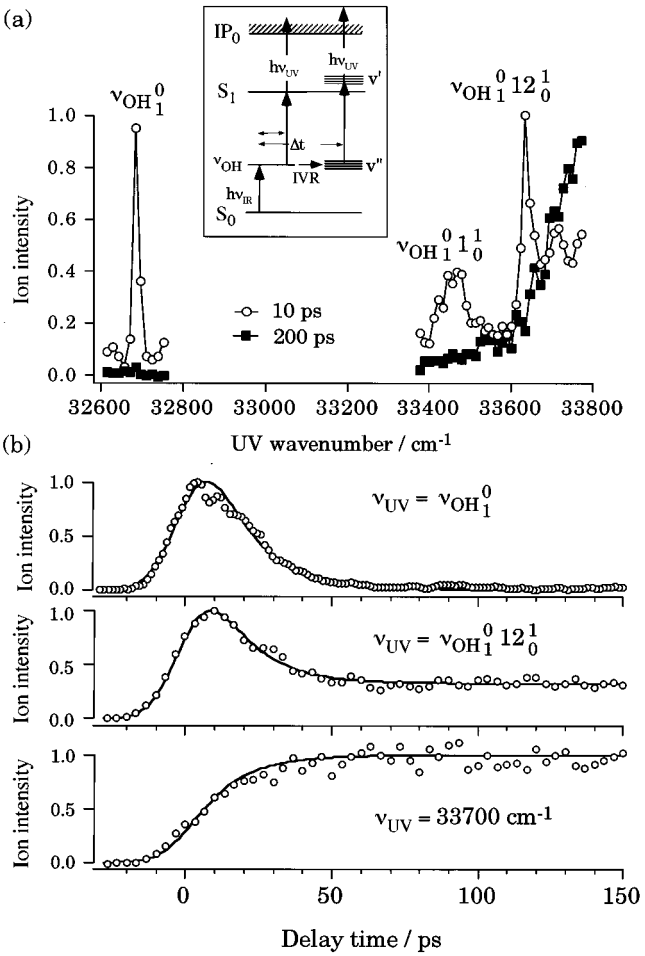

Figure 3. (a) 1+1 REMPI spectrum of phenol obtained at delay times of 10 and 200 ps after the IR excitation to the OH stretching vibration of phenol. (b) Transient profiles of the ν_{OH1}^0 and $\nu_{OH1}^0 12_0^1$ (1+1) REMPI signals, and the ion signal monitored at 33700 cm^{-1}. Solid curves are the convoluted ones. See text.

UV pulses. The figure shows that the $\nu_{OH_1}^0$ and the $\nu_{OH1}^0 12_0^1$ bands decays until 50 ps, though the latter band does not return to zero. In contrast, the ion signal monitored at 33700 cm^{-1} shows a distinct rise until 50 ps and approaches to a fixed value. By deconvolution, the $\nu_{OH_1}^0$ band decay curve was well reproduced with a single-exponential decay curve having τ_{decay} = 14 ps, as shown by a solid curve. The transient profiles of the $\nu_{OH1}^0 12_0^1$ band and the ion signal monitored at 33700 cm^{-1}, on the other hand, were reproduced by the combination of a decay and a rise as follows:

$$I(t) = A \exp(-t/\tau_{decay}) + B\{1 - \exp(-t/\tau_{rise})\}$$

Here, we used the same lifetime for the rise and the decay components, that is, $\tau_{rise} = \tau_{decay} = 14$ ps. The decay curve of the $\nu_{OH_1}^0 12_0^1$ band was well fitted by adjusting $A/B = 4.0$, and the rise curve of the 33700 cm^{-1} signal was fitted with $A/B = 0.14$. The reason they are expressed by the two components is that two electronic transitions, resonant transition of the OH stretching level and the broad background transition, are overlapped in those bands. As seen in Figure 3a, the $\nu_{OH_1}^0 12_0^1$ band is overlapped with weak broad background. Even though the signal at 33700 cm^{-1} mainly involves the broad background transitions, the position overlaps with the $\nu_{OH_1}^0 18_0^1$ transition.[66] The coincidence of the decay of the pumped level with the rise of the broad background transition strongly suggests that the broad background is the transitions from the redistributed levels

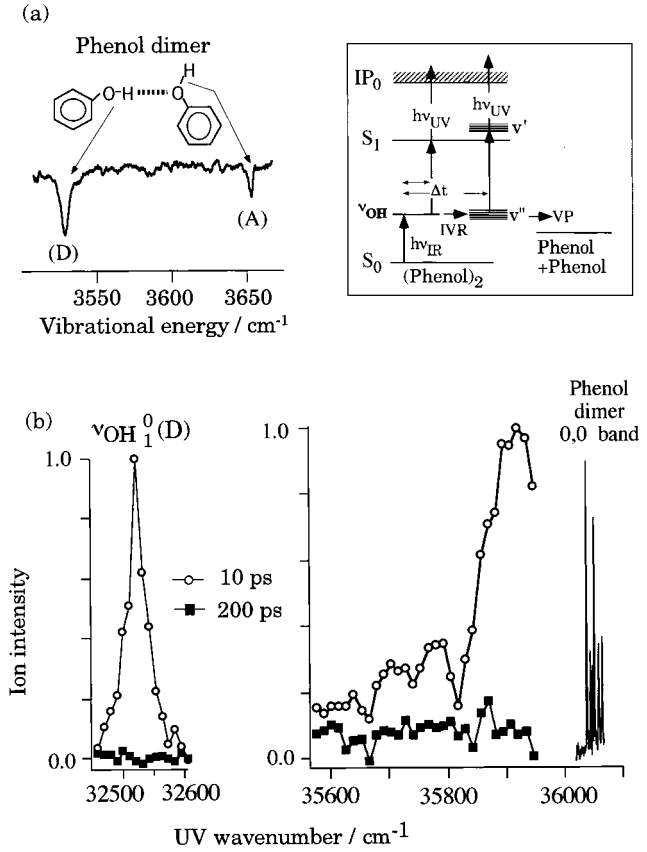

Figure 4. (a) Ionization-detected IR spectrum of the phenol dimer. The spectrum was obtained by monitoring the (0,0) band REMPI signal of the dimer while scanning the IR frequency. (b) 1+1 REMPI spectra obtained at delay times of 10 and 200 ps after the IR excitation to the donor OH stretching vibration of the phenol dimer. The sharp bands at 36040 cm^{-1} are the 1+1 REMPI spectrum of the phenol dimer in the 0,0 band region, observed by a nanosecond laser.

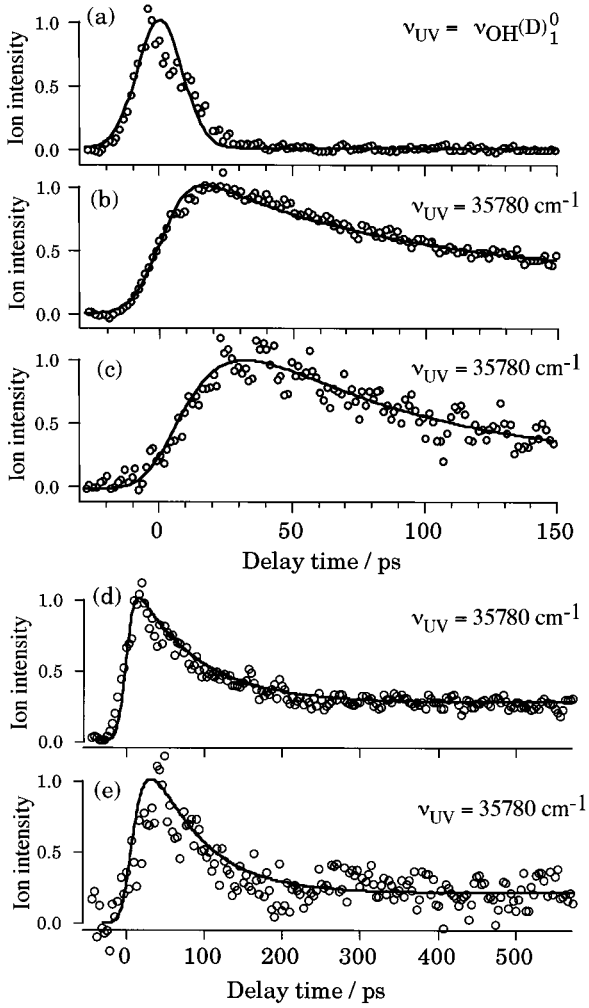

Figure 5. Transient profiles of (a) donor ν_{OH1}^0 band (b) ion signal monitored at 35780 cm^{-1} , after the IR pumping to the donor OH stretching vibration of phenol dimer. (c) Transient profile of the ion signal monitored at 35780 cm^{-1} after the IR pumping to the acceptor OH stretching vibration. (d), (e) Transient profile of the ion signal monitored at 35780 cm^{-1} in the longer time scale (0−500 ps) after the IR pumping to the donor OH stretching and the acceptor OH stretching vibrations, respectively. Solid curves were convoluted ones by setting (a) $\tau_{decay} = 5$ ps, (b), (d) $\tau_{rise} = 5$ps and $\tau_{decay} = 89$ ps, and (c),(e) $\tau_{rise} = 14$ ps and $\tau_{decay} = 55$ ps, respectively.

from initially prepared OH stretching level, and IVR of OH stretching level for bare phenol occurs with $\tau_{IVR} = 14$ ps, corresponding $k_{IVR} = 1/\tau_{IVR} = 7.1 \times 10^{10}$ s^{-1}.

2. Phenol Dimer. Figure 4a shows the ionization-detected IR spectrum of phenol dimer obtained by nanosecond IR−UV double resonance spectroscopy.[2] The spectrum was recorded by scanning the IR laser frequency, while monitoring the dimer S_1-S_0 REMPI signal by the UV laser. Here the IR pulse was introduced 50 ns prior to the UV pulse. As seen in the figure, the spectrum of the phenol dimer exhibits a H-bonded (or a donor) OH stretching vibration at 3530 cm^{-1}, and a free (or an acceptor) OH stretching vibration at 3654 cm^{-1}.[2] It is seen that the bandwidth of the donor OH stretching vibration is broader than that of the acceptor OH stretching vibration. Earlier, Felker's group measured the Raman spectra of the OH stretch vibrations of phenol dimer and reported that the width of the donor OH stretch was 2.4 cm^{-1}, while that of the acceptor OH was 1.2 cm^{-1}, suggesting a shorter lifetime of the former vibration.[63] As was mentioned previously, it should be also noted that the energies of both OH stretching vibrations are large enough to break the H-bond, since the H-bonding energy of the dimer is estimated to be 2100−2500 cm^{-1}.[67] Thus, both IVR and vibrational predissociation (VP) can contribute the relaxation process of the prepared level, though it is not clear which process is mainly responsible for the broadening of the bandwidths. So, we measured the time evolution of the OH stretching level as well as the energy redistributed vibrational levels by IR−UV pump−probe spectroscopy.

Figure 4b shows the 1+1 REMPI spectra of phenol dimer observed at delay times of 10 and 200 ps after the IR pumping of the donor OH stretching level at 3530 cm^{-1}. The spectrum measured at the delay time of 10 ps consists of a sharp band at 32520 cm^{-1}, which is assigned to the donor ν_{OH1}^0 electronic transition of the dimer, hereafter we use $\nu_{OH}(D)_1^0$, and intense broad background in the higher frequency region, indicating that IVR occurs very rapidly for the donor OH excitation. In the spectrum observed at 200 ps delay time, not only the sharp $\nu_{OH}(D)_1^0$ band completely disappears, but also the intensity of the broad background becomes very weak. The decrease of the broad background intensity was not observed for phenol monomer, and it can be explained by VP of IVR redistributed levels.

Figure 5, parts a and b, shows the time evolution of the $\nu_{OH}(D)_1^0$ band at 32520 cm^{-1}, and the background signal intensity monitored at 35780 cm^{-1} , respectively, for the delay time until 150 ps. The $\nu_{OH}(D)_1^0$ band exhibits very fast decay, and the convoluted decay curve by setting $\tau_{decay} = 5$ ps is shown in Figure 5a. Since similar decay curves were obtained by assuming a shorter lifetime than 5 ps, τ_{IVR} ($= \tau_{decay}$) is roughly

estimated to be equal to or shorter than 5 ps, that is $k_{IVR} \geq 2 \times 10^{11}$ s^{-1}. Thus, IVR for the donor OH stretching level of the dimer occurs much faster than that of bare phenol. The transient profile of the background signal intensity monitored at 35780 cm^{-1} was reproduced by a convolution with $\tau_{rise} = 5$ ps and a decay lifetime of $\tau_{decay} = 89$ ps. Since the decay of the pumped level coincides with the rise of the energy redistributed levels, it is concluded IVR occurs within 5 ps in the case of the donor OH stretching level excitation. The subsequent decay ($\tau_{decay} =$ 89 ps) of the broad background signal is due to VP of the redistributed levels. Thus, VP occurs after IVR with the lifetime more than 17 times slower than that of IVR.

Figure 5d shows the decay of the background signal monitored at 35780 cm^{-1} in a longer time scale. As seen in the figure, the signal does not return to zero, but evolves to a constant value even at the 500 ps delay time. This indicates that there must be a very slow process in addition to the VP decay, which may be due to an incomplete energy randomization of IVR or due to the existence of redistributed levels which are not coupled to the VP process.

A similar experiment was carried out for the acceptor OH stretching level (3654 cm^{-1}) of the dimer. In the case of the acceptor OH excitation, we could not observe the resonant transitions from the pumped OH stretching level, which is probably due to the weakness of the electronic transition of the accepting site and to the overlap with the transition of the donor site. However, a broad structureless background was easily observed similar to the case of the donor OH excitation. Figure 5c shows the time profile of the broad background signal after the acceptor OH excitation. As seen in the figure, the rise of the background signal intensity is slower than that of the donor OH excitation, while the decay is faster. The transient profile was well fitted by the convolution using a rise time of $\tau_{rise} =$ 14 ps and a decay time of $\tau_{decay} = 55$ ps, as shown by a solid curve. Thus, the acceptor OH stretching level exhibits slower IVR decay (14 ps) than that of the donor OH stretching level (5 ps). The faster IVR of the donor site OH stretching level is due to the fact that is strongly coupled with the intermolecular modes and the vibrational energy randomization occurs very fast in the whole cluster. On the other hand, the fact that the IVR lifetime of OH stretching level of the acceptor site is very similar to that of bare phenol OH stretching level suggests that the coupling between the acceptor OH stretching level and the intermolecular vibrational modes is very weak in the dimer, and the initial energy randomization occurs only within phenol in the acceptor site. Figure 5e shows the decay of the signal at longer time scale. Similar to the case of the donor OH stretch excitation, the signal does not come back to zero, representing the presence of slower decay process similar to the case of donor OH stretching vibration.

For VP, the lifetime from the acceptor OH stretching level ($\tau_{VP} = 55$ ps) was shorter than that from the donor OH stretching level ($\tau_{VP} = 89$ ps). It should be noted that this behavior is opposite to that observed in HF dimer, where the VP lifetime of the H-bonded HF stretching vibration is 40 times shorter than that of the free HF stretching vibration. The difference between the two systems might be explained by the difference of the coupling scheme, that is, VP in HF dimer occurs via the direct coupling between the HF stretch and the dissociation continuum, while VP in the phenol dimer occurs sequentially after IVR. The IVR → VP sequential process was also observed in several clusters in the S_1 state, such as phenol−benzene,[31] anthracene−Ar_n,[33] aniline−CH_4,[38] etc., though their rates depend on the vibrational energies and on the types of the clusters.

At this point, we should comment on the comparison of the present results with those of our pervious work,[54] where we applied similar IR−UV pump spectroscopy with nanosecond laser pulses. We reported that IVR occurs in a few nanoseconds for bare phenol, and its decay profile can be described by an intermediate coupling scheme. On the other hand, the present picosecond experiment has presented much faster IVR time profile with a single-exponential decay. Thus, it looks as if the two experiments are providing contradicting results.

The difference of the two results can be explained by the following. In the nanosecond laser experiment, the laser bandwidth of was ∼0.1 cm^{-1}, which was not large enough to excite all the levels having the OH stretching level character so that the time evolution might occur only within the limited levels. Table 1 lists the bandwidths of the OH stretching level obtained by the group of Felker the stimulated Raman spectroscopy[52], and those obtained from the present work. As seen in the table, both the Raman bandwidth and the present measurements give the width of the OH stretching level as being much broader than the width of the nanosecond laser. Therefore the slow decay observed in the nanosecond experiment is due to the incomplete excitation of the levels having the OH stretch vibrational character. In the table, the bandwidths estimated in the present work are smaller than those reported by Raman spectroscopic measurement. At this moment, we do not have a clear answer for this discrepancy.

In summary, picosecond time-resolved IR−UV pump−probe spectroscopy has been applied to the investigation of mode-specific IVR of the OH stretching vibration of phenol and its clusters in the S_0 state. It was found that IVR of the OH stretch vibration of bare phenol occurs with a lifetime of 14 ps. In the phenol dimer, a remarkable acceleration of IVR rate was observed for the donor site OH stretch, while the IVR rate of the acceptor site OH was almost equal to that of bare phenol. In addition, it was found that vibrational predissociation occurs sequentially after IVR. For the future work, an extension to larger size clusters will be very interesting to examine a cage effect of the dissociation process.

Acknowledgment. The authors thank Prof. Domen and Dr. Wada at the Tokyo Institute of Technology for their advice in designing the laser system. This work is partially supported by the Grant-in-Aids for Scientific Research (No. 12640483) by Japan Society for the Promotion of Science. T.E. also acknowledges the support from the Sumitomo Foundation.

References and Notes

(1) Tanabe, S.; Ebata, T.; Fujii, M.; Mikami, N. *Chem. Phys. Lett.* **1993**, *215*, 347.
(2) Ebata, T.; Watanabe, T.; Mikami, N. *J. Phys. Chem.* **1995**, *99*, 5763.
(3) Iwasaki, A.; Fujii, A.; Watanabe, T.; Ebata, T.; Mikami, N. *J. Phys. Chem.* **1996**, *100*, 16053.
(4) Watanabe, T.; Ebata, T.; Tanabe, S.; Mikami, N. *J. Chem. Phys.* **1996**, *105*, 408.
(5) Mitsuzuka, A.; Fujii, A.; Ebata, T.; Mikami, N. *J. Chem. Phys.* **1996**, *105*, 2618.
(6) Matsumoto, Y.; Ebata, T.; Mikami, N. *J. Chem. Phys.* **1998**, *109*, 6303.
(7) Mitsuzuka, A.; Fujii, A.; Ebata, T.; Mikami, N. *J. Phys. Chem. A* **1998**, *102*, 9779.
(8) Matsuda, Y.; Ebata, T.; Mikami, N. *J. Chem. Phys.* **1999**, *110*, 8397.
(9) Ishikawa, S.; Ebata, T.; Mikami, N. *J. Chem. Phys.* **1999**, *110*, 9504.
(10) Guchhait, N.; Ebata, T.; Mikami, N. *J. Chem. Phys.* **1999**, *111*, 8438.
(11) Guchhait, N.; Ebata, T.; Mikami, N. *J. Am. Chem. Soc.* **1999**, *121*, 5705.
(12) Matsuda, Y.; Ebata, T.; Mikami, N. *J. Chem. Phys.* **2000**, *113*, 573.
(13) Matsumoto, Y.; Ebata, T.; Mikami, N. *J. Mol. Struct.* **2000**, *552*, 257.

(14) Matsuda, Y.; Ebata, T.; Mikami, N. *J. Phys. Chem. A*, in press.
(15) Fredericks, S. Y.; Jordan, K. D.; Zwier, T. S. *J. Phys. Chem.* **1996**, *100*, 7810.
(16) Hagemeister, F. C.; Gruenloh, C. J.; Zwier, T. S. *Chem. Phys.* **1998**, *239*, 83.
(17) Florio, G. M.; Grenloh, C. J.; Quimpo, R. C. Zwier, T. S. *J. Chem. Phys.* **2000**, *113*, 11143.
(18) Barth, H. D.; Buchhold, K.; Djafari, S.; Reimann, B.; Lommatzsch, U.; Brutschy, B. *Chem. Phys.* **1998**, *239*, 49.
(19) Tarakeshwar, P.; Kim, K. S.; Brutschy, B. *J. Chem. Phys.* **1999**, *110*, 8501.
(20) Brutschy, B. *Chem. Rev.* **2000**, *100*, 3891.
(21) Buchhold, K.; Reinmann, B.; Djafari, S.; Barth, H. D.; Brutschy, B.; Tarakeshwar, P.; Kim, K. S. *J. Chem. Phys.* **2000**, *112*, 1844.
(22) Janzen, Ch.; Spangenberg, D.; Roth, W.; Kleinermanns, K. *J. Chem. Phys.* **1999**, *110*, 9898.
(23) Palmer, P. M.; Chen, Y.; Topp, M. R. Chem. Phys. Lett. **2000**, *318*, 440.
(24) Robertson, E. G.; Hockridge, M. R.; Jelfs, P. D.; Simons, J. P. *J. Phys. Chem. A* **2000**, *104*, 11714.
(25) De Souza, A. M.; Kaur, D.; Perry, D. S. *J. Chem. Phys.* **1988**, *88*, 4549.
(26) Bethardy, G. A.; Perry, D. S. *J. Chem. Phys.* **1993**, *98*, 6651.
(27) Lehmann, K. K.; Pate, B. H.; Scoles, G. *J. Chem. Phys.* **1990**, *93*, 2152.
(28) Gambogi, J. E.; Lehmann, K. K.; Pate, B. H.; Scoles, G.; Yang, J. *J. Chem. Phys.* **1993**, *98*, 1748.
(29) Callegari, A.; Merker, U.; Engels, P.; Srivastava, H. K.; Lehmann, K. K.; Scoles, G. *J. Chem. Phys.* **2000**, *113*, 10583.
(30) Miller, R. E. In *Structure and dynamics of weakly bound molecular complexes*; Weber, A., Ed.; NATO ASI series, D. Reidel Publishing Company: Dordrecht/Boston/Lancaster/Tokyo, 1986; pp 131−140.
(31) Huang, Z. S.; Miller, R. E. *J. Chem. Phys.* **1989**, 91, 6613.
(32) Nesbitt, D. J. *Annu. Rev. Phys. Chem.* **1994**, *45*, 367.
(33) Nesbitt, D. J. In *Reaction dynamics in clusters and condensed phases*; ed. by Jortner, J., Leveine, R. D., and Pullman, B., Eds.; *Proceedings of the 26th Jerusalem symposium on quantum chemistry and biology*; Kluwer Academic Publishers: Dordrecht/Boston/ London, 1993; pp 137−152.
(34) Bevan. J. W. *Structure and dynamics of weakly bound molecular complexes*; Weber, A., Ed.; NATO ASI series, D. Reidel Publishing Company: Dordrecht/Boston/Lancaster/Tokyo, 1986; pp 149−169.
(35) Knee, J. L.; Khundkar, L. R.; Zewail, A. Z. *J. Chem. Phys.* **1987**, *87*, 115.
(36) Semmes, D. H.; Baskin, J. S.; Zewail, A. H. *J. Chem. Phys.* **1990**, *92*, 3359.
(37) Heikal, A.; Banãres, L.; Semmes, D. H.; Zewail, A. H. *Chem. Phys.* **1991**, *157*, 231.
(38) Lienau, C.; Heikal, A. A.; Zewail, A. H. *Chem. Phys.* **1993**, *175*, 171.
(39) Kaziska, A. J.; Topp, M. R. *Chem. Phys. Lett.* **1991**, *180*, 423.
(40) Kaziska, A. J.; Wittmeyer, S. A.; Topp, M. R. *J. Phys. Chem.* **1991**, *95*, 3663.
(41) Topp, M. R. *Int. Rev. Phys. Chem.* **1993**, *12*, 149.
(42) Bernstein, E. R. In *Dynamics of Polyatomic van der Waals Complexes*; Halberstadt, N., Janda, K. C., Eds.; Plenum Press: New York, 1990; pp 295−320.
(43) Smith, P. G.; McDonald, J. D. *J. Chem. Phys.* **1990**, *92*, 1004.
(44) Lakshminarayan, C.; Knee, J. L. *J. Phys. Chem.* **1990**, *94*, 2673.
(45) Connell, L. L.; Ohline, S. M.; Joireman, P. W.; Corcoran, T. C.; Felker, P. M. *J. Phys. Chem.* **1992**, *96*, 2585.
(46) Gerhards, M.; Kleinermanns, K. *J. Chem. Phys.* **1995**, *103*, 7392.
(47) Berden, G.; Leo Meerts, W.; Schmitt, M.; Kleinermanns, K. *J. Chem. Phys.* **1996**, *104*, 972.
(48) Gerhards, M.; Schmitt, M.; Kleinermanns, K.; Sthal, W. *J. Chem. Phys.* **1996**, *104*, 967.
(49) Janzen, Ch.; Spangenberg, D.; Roth, W.; Kleinermanns, K. *J. Chem. Phys.* **1999**, *110*, 9898.
(50) Schütz, M.; Bürgi, T.; Leutwyler, S. *J. Chem. Phys.* **1993**, *198*, 3763.
(51) Bürgi, T.; Schütz, M.; Leutwyler, S. *J. Chem. Phys.* **1995**, *103*, 6350.
(52) Sur, A.; Johnson, P. M. *J. Chem. Phys.* **1986**, *84*, 1206.
(53) Lipert, R.; Bermudez, G.; Colson, S. D. *J. Phys. Chem.* **1988**, *92*, 3801.
(54) Lipert, R.; Colson, S. D. *J. Phys. Chem.* **1989**, *93*, 135.
(55) Lipert, R.; Colson, S. D. *J. Phys. Chem.* **1990**, *94*, 2358.
(56) Syage, J. A.; Steadman, J. *J. Chem. Phys.* **1991**, *95*, 2497.
(57) Steadman, J.; Syage, J. A. *J. Am. Chem. Soc.* **1991**, *113*, 6786.
(58) Steadman, J.; Syage, J. A. *J. Phys. Chem.* **1991**, *95*, 10326.
(59) Pino, G. A.; Dedonder-Lardeux, C.; Jouvet, C.; Martrenchard, S.; Solgadi, D. *J. Chem. Phys.* **1999**, *111*, 10747.
(60) Pino, G.; Gregoire, G.; Dedonder-Lardeux, C.; Jouvet, C.; Martrenchard, S.; Solgadi, D. *Phys. Chem. Chem. Phys.* **2000**, *2*, 893.
(61) Ishiuchi, H.; Saeki, M.; Sakai, M.; Fujii, M. *Chem. Phys. Lett.* **2000**, *322*, 27.
(62) Ebata, T.; Furukawa, M.; Suzuki, T.; Ito, M. *J. Opt. Soc. Am. B* **1990**, *7*, 1890.
(63) Hartland, G. V.; Henson, B. F.; Venturo, V. A.; Felker, P. M. *J. Phys. Chem.* **1992**, *96*, 1164.
(64) Ishiuchi, S.; Shitomi, H.; Takazawa, K.; Fujii, M. *Chem. Phys. Lett.* **1998**, *283*, 243.
(65) Ebata, T.; Iwasaki, A.; Mikami, N. *J. Phys. Chem. A* **2000**, *104*, 7974.
(66) Abe, H.; Mikami, N.; Ito, M. *J. Phys. Chem.* **1982**, *86*, 1768.
(67) Couty, A.; Mons, M.; Dimicoli, I.; Piuzzi, F.; Brenner, V.; Millie, P. *J. Phys. Chem.* A **1998**, *102*, 4890.